

# SHIP WAKE DETECTION IN SAR IMAGERY

## 1 INTRODUCTION

The ability to accurately monitor ships is vital to ensuring the safety and security of our waters. Ship traffic surveillance relies on a combination of Automatic Identification System (AIS) and RADAR. The Synthetic Aperture Radar (SAR) can be used to complement the limited and vulnerable AIS, over a wider range by synthesizing a larger aperture. By nature of transmitting radio waves, SAR also produces all-weather and day/night imaging, which is advantageous for effective surveillance.

## 2 BACKGROUND

Ships have high Radar Cross Sections (RCS) and usually appear as bright features in SAR imagery due to strong corner reflectors on their hulls, causing its backscatter echo to be much stronger than that of sea. When ships move through the sea, ship wakes are formed due to the displacement in fluid caused by the ship, resulting in the formation of a region of low pressure behind it. Ship wakes can establish a ship's status (i.e. presence, bearing and velocity) more accurately and reliably than the ship itself. This is due to the wake's pronounced shape and length. However, ship wake detection presents a challenge because there is a great variety of wakes that could appear in SAR imagery, namely: Kelvin wakes, narrow-V wakes, internal wakes and turbulent wakes [1]. According to a study by *Eldhuset* [2], turbulent wakes are the most common wake-type present in SAR images, with 85% of 200 wake-like features in SEASAT L-band imagery and 80% of 180 ERS-1 C-band images exhibiting turbulent wakes. Turbulent wakes appear dark in SAR imagery as they are smoother in comparison to the wind-roughened surrounding sea. In order to not rule out detection of other bright wakes in the absence of the dark turbulent wake, the algorithm is constructed to detect both bright and dark ship wakes in SAR imagery. In SAR imagery, moving ships are often displaced from their wakes as a result of Doppler shift. This offset can be used to calculate the ship's velocity to aid our proximity criteria.

$$V_{ship} = \frac{V_s \Delta x}{R \cos \beta}$$

$\Delta x$ : cross-range displacement of ship from wake,

$R$ : range of the radar (at center time) to target,

$V_s$ : platform velocity,

$V_{ship}$ : ship's estimated ground velocity,

$\beta$ : angle between ship velocity vector and radar beam.

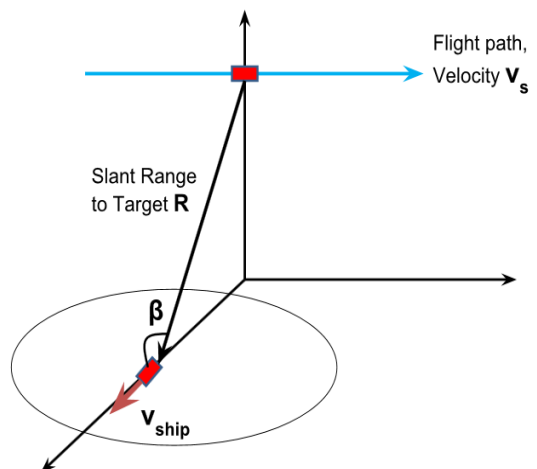


Figure 1: Diagram illustrating the equation for ship velocity estimation.

### 3 METHODOLOGY

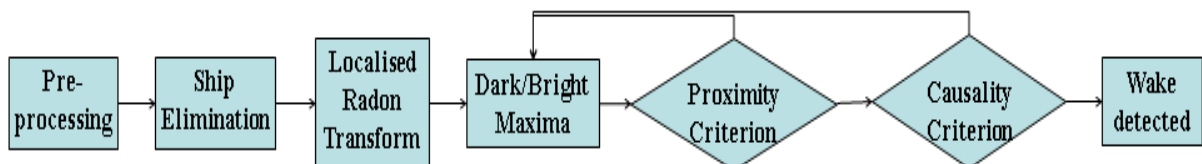


Figure 2: High-level workflow.

The objective of our algorithm is to detect the correct wake, or lack thereof, of which features can be used to establish properties of its respective ship. Various criteria and filters are applied to observe their effect on detection rates and processing requirements. Corresponding satellite particulars are also manipulated to describe ship particulars on actual scale.

#### 3.1 Pre-processing

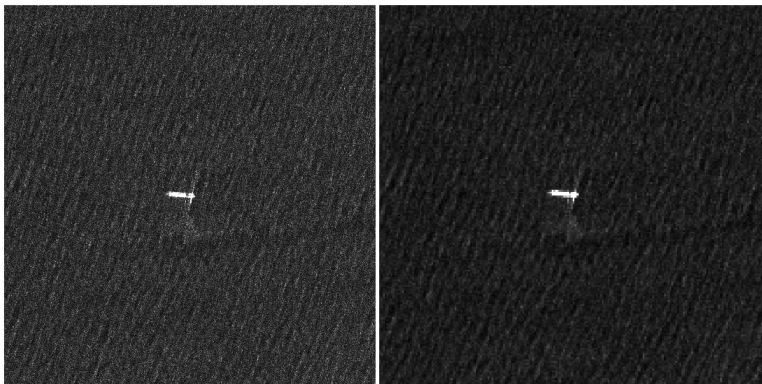


Figure 3: Original chip (Scenario 1). Figure 4: After block processing.

##### 3.1.1 Block Processing

By thresholding the SAR image, bright ship candidates are selected and centred in "chips". After which, block processing is employed to decrease processing time and speckle noise.

#### 3.1.2 Image Treatment: Normalising Filter

Certain SAR images possess a varying intensity gradient due to system effects affecting pixel distributions, thus obscuring wake features. In such extreme cases, normalising the image is necessary to cancel sea clutter in order for subsequent criteria to function effectively. This filter applies a horizontal classic median filter to reduce noise while preserving edges.



#### 3.2 Ship Elimination: Sea Threshold

The ship's high intensity pixels overshadow the wake and affect image distribution. As the radar cross section (RCS) of a ship is higher than that of its surroundings, there is large enough difference between pixel values to separate the ship and the sea using an appropriate threshold. While optimal images allow  $4 \times \text{median}$ , lower thresholds (e.g.  $2 \times \text{median}$ ) are chosen to accommodate noisier images.

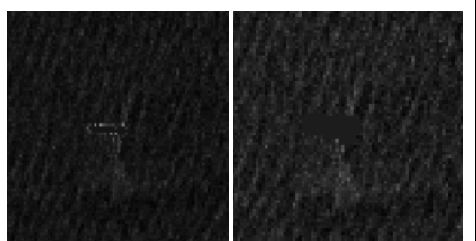


Figure 5: After ship elimination (with residual bright edges)

Figure 6: After ship elimination with dilation.

##### 3.2.1 Morphology – Dilation

Morphological dilation is then applied to overlap residue bright ship edges in order to prevent similar overshadowing.



### 3.3 Localised Radon Transform

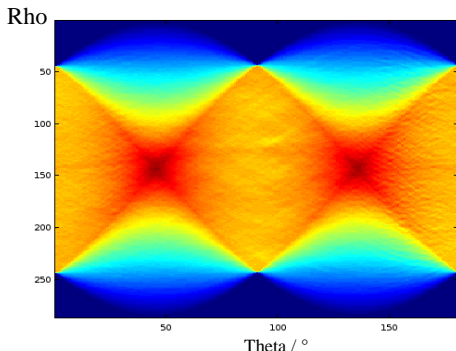


Figure 7: Radon transform of chip with wake only (Fig.7).

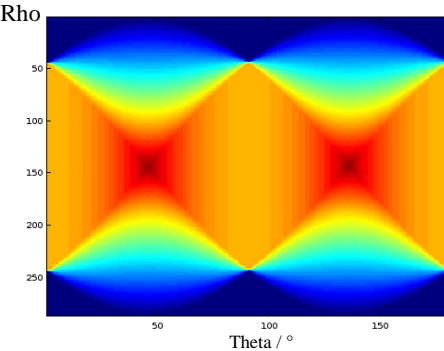


Figure 8: Radon transform of median of chip (background).

The chips are then Radon transformed to detect linear features. The Radon transform is an integration of points along a line into a parametric space, accentuating linear features in the process. Hence, it is the most suitable tool for our purpose of

ship wake detection because ship wakes are usually linear structures with a constant intensity (causing curved wakes to fail detection). This process averages every wake line, diminishing noise perturbations, improving the signal-to-noise ratio (SNR). However, other longer or darker linear features that have larger integration values can overshadow the wake in the Radon space.

Furthermore, the inverse Radon transform can also be applied to reconstruct the wake back onto the image.

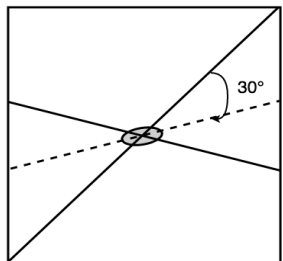


Figure 10: Diagram illustrating Limited Angles filter.

#### 3.3.1 Limited Angles Filter ( $\pm 30^\circ$ of ship)

Obtaining ship heading from wakes is more reliable than the ship due to ship's smaller size, making it vulnerable to noise. However, we suggest that the ship's heading can still be used to restrict range of radon angles ( $\pm 30^\circ$ ), which was obtained from radon of threshold the filtered ship itself. Limiting Radon angles rejects many false values, and lowers the maxima and breakpoints observed.

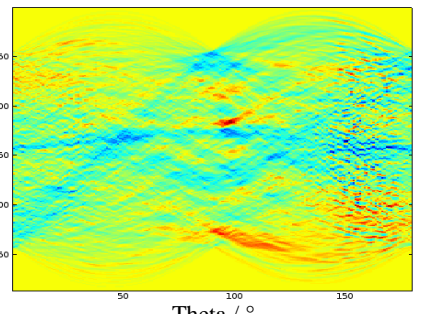


Figure 9: Radon transform of only the dark wake, obtained by Fig. 10 minus Fig. 9.



### 3.4 Proximity Criterion

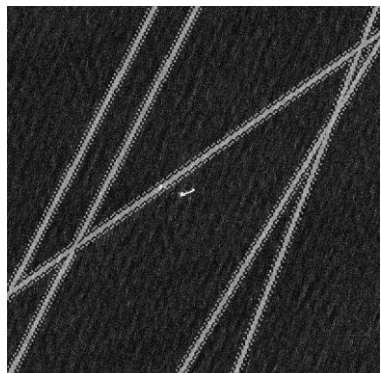


Figure 11: A chip showing rejected lines and correct wake.

The maximum Doppler displacement of wake from ship can be used to eliminate false lines by the evident fact that a ship cannot be displaced too far from its wake. The corresponding maximum velocity ( $17.182\text{ms}^{-1}$ ) was observed from MarineTraffic [3] over a period of 30 days. From the Radon transform, more prominent lines, which possess brighter maxima, are detected, and then checked against this Proximity Criterion. The process is repeated until an adequately near wake line is successfully detected, or terminated at established breakpoints (i.e. once the median is reached). Other breakpoints can be established by comparing data of chips

containing ships with and without wakes. A small patch around a rejected point in the Radon transform space is also removed to minimise selection of similar rejected lines. An appropriately low maximum ( $N$ ) is required to reject false candidates while including possible wakes. Scherbakov [4] noted that prominent wakes are almost always detected, whereas it is difficult to determine validity of results after rejecting many maxima.



### 3.5 Causality Criterion

Turbulent wakes are formed only on one side of a displaced ship. Scherbakov suggests the Causality Criterion to exploit this feature by dividing the line containing the detected wake along the centre (40% to 60%) and comparing the distributions of the two parts of the line.

$$\sigma_{\mu_i} = \frac{\sigma}{\sqrt{N_i}}, i = \{1, 2\}, \quad K = \frac{|\mu_1 - \mu_2|}{\sqrt{\sigma_{\mu_1}^2 + \sigma_{\mu_2}^2}} > R(\alpha)$$

$\mu$ : mean,  $\sigma$ : standard deviation,  $N$ : pixel count,  $K(\alpha)$ : normal distribution (eg  $K(0.05) = 1.96$ )

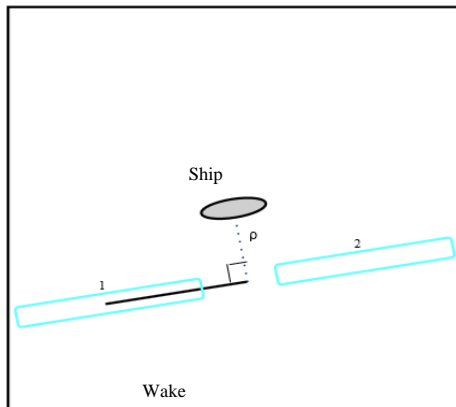


Figure 12: Diagram illustrating the Causality Criterion.

However, such reliance on distribution makes the Causality Criterion susceptible to noise and SAR's varying intensity gradient. Furthermore, long wakes stretching for an entire half of the image can also result in lower  $R$  (or  $K$ ) values due to decreased fluctuation and even distribution. Weak wakes also cause minimal difference in the pixel intensity when compared to the sea, resulting in little to no effect on the standard deviation of pixels. We aimed to observe threshold of the criterion and how additional filters could improve  $K$  values.



**Wake detected**

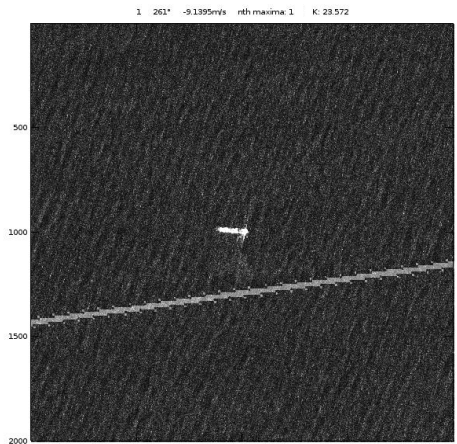


Figure 13: Chip with wake mapped back onto it.

## 4 RESULTS & DISCUSSION

### 4.1 Input

The algorithm was tested on two SAR images to determine its effectiveness. The first dataset was taken in the Straits of Gibraltar, with 11 ship chips, 10 sea chips,  $3 \times 3$ m resolution, and 1.25m pixel spacing [Fig. 15]. The second dataset was taken in the Malacca Strait, with 30 chip ships, 15m pixel spacing [Fig. 16]. The algorithm is written in GNU Octave.

### 4.2 Output

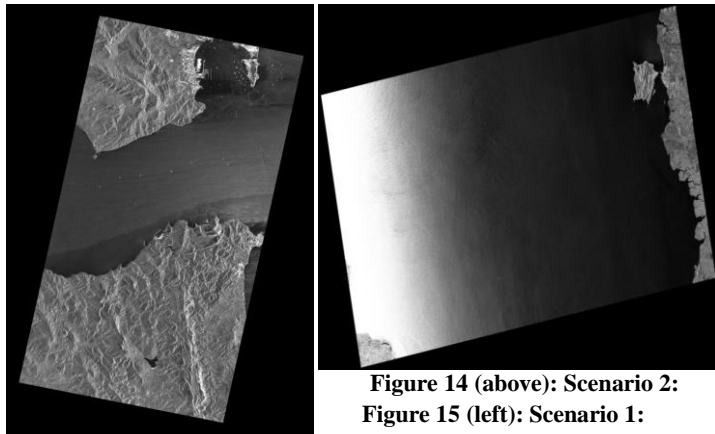


**Figure 14 (above): Scenario 2:**  
**Figure 15 (left): Scenario 1:**

Since AIS data corresponding to the SAR images' timing could not be obtained, the detected wake was overlaid onto the image for comparison and verification with actual wake. Given the macro perspective, pixel-level accuracy of the detected wake could not be determined visually. This gives rise to the need for  $N$  maxima and  $K$  values thresholds. In this case, the  $N < 6$  and  $K > 7.29$

were set as the threshold values using their best separation from the scatter plot.

Algorithm \ Visual	Positive Wakes	Negative wakes
Detected as wakes	Scen1: 11 of 11 + Scen2: 17 of 21 87.5% (28 of 32)	Scen1: 0 of 10 + Scen2 0 of 7 0% (0 of 17)
Detected as no wakes	Scen1: 0 of 11 + Scen2: 4 of 21 12.5% (4 of 32)	Scen1 10 of 10 + Scen2 7 of 7 100% (17 of 17)

Positive wakes: wakes that appeared to be correctly detected using visual inspection.

Negative wakes: wakes that were non-existent or curved (i.e. undetectable).

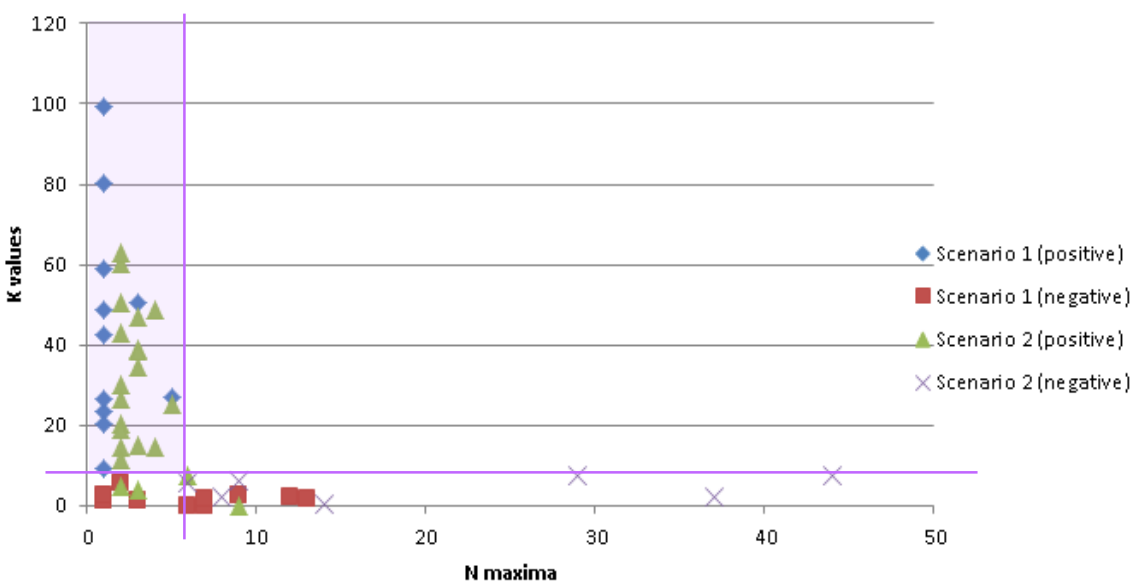


**Figure 16:** Scatter plot of  $K$  values against  $N$  maxima obtained.

## 5 DISCUSSION

### 5.1 Objectives

Besides automating ship wake detection, the algorithm should also produce reliable indicators of success or failure. The two vastly different scenarios were intentionally chosen in order to carry out comparison of the  $N$  maxima (Proximity Criterion) and  $K$  values (Causality Criterion) obtained from their chips. We aim to observe possible trends between that of chips with and without wakes, and by doing so determine the threshold for the respective filters. This also presents the opportunity to ascertain the importance, of lack thereof, of the criteria. Scenario 1 (Fig. 15) contains favourable background conditions with minimal noise and small pixel spacing. On the other hand, Scenario 2 (Fig. 16) is more challenging as the image is affected by a multitude of system effects that have resulted in a varying intensity gradient along the travel path. Moreover, the image's large pixel spacing makes it difficult to accurately determine ship velocities.

### 5.2 Analysis of Results

Upon visual inspection of the wakes mapped back onto the chips, it appears that the algorithm has succeeded in detecting all chips containing wakes for both Scenarios 1 and 2. However, verification using the  $N$  maxima and  $K$  values thresholds proves otherwise.

#### 5.2.1 Scenario 1

Small pixel spacing allows for deduction of an accurate velocity for most ships using the Doppler shift. The calculated bearing of most ships implies that they are moving out of the Port of Gibraltar. The Proximity Criterion appears to have successfully rejected false candidates within low maxima for all chips containing wakes, with 81.8% (9 of 11) at  $N = 1$ . This is in contrast to the chips containing only noise, with 60% (6 of 10) at  $N < 5$ . This is promising data, allowing for the conclusion that an appropriately low maximum offset ensures that the algorithm effectively rejects false cases and vice versa. However, it is apparent that this alone is inadequate verification of a wake's presence. The Causality Criterion results in 90.9% (10 of 11) of  $K$  values in the double digits. Even some chips with low  $K$  values are still above suggested 95% certainty of  $K(0.05) = 1.96$  and still much higher than that of the chip containing only noise, with 100% of  $K$  values  $< 2.5$ . Thus, all wakes achieved detection. In this case, setting a  $K$  values threshold is sufficient to ascertain a wake's presence, proving to be the more effective and reliable measure.

#### 5.2.2 Scenario 2

The image was run through all three of the various filters. Out of the 30 chips sampled, 8 chips were considered negatives, as their wakes are non-existent, curved or weak, making them impossible to detect. Such extreme cases will too, be used to validate discussions of  $N$  maxima and  $K$  thresholds. Following the addition of the Normalising Filter, the varying intensity gradient has been removed, allowing for reliable comparison of  $K$  values. In comparison to Scenario 1, the utilization of the selected thresholds in this scenario has resulted in

the rejection of three chips which originally appeared to have passed. Usage of the  $N$  maxima threshold proves effective in determining the wake's presence, eliminating any chips with  $N > 5$ . This is favourable data, as all 8 of the negative chips failed this threshold. Results of the  $K$  values threshold is too, promising, eliminating all negative chips as well as 3 chips which appeared to have passed originally.

### 5.3 Importance of the Thresholds

These results have proven the effectiveness of the  $N$  maxima and  $K$  values thresholds in determining the presence of a wake. It is interesting to note that in some cases, only using one threshold is sufficient, but in noisy conditions where the  $K$  values may fluctuate (i.e. Scenario 2), employing the use of both thresholds is necessary to eliminate false alarms.

### 5.4 Limitations and Further Work

Currently, the algorithm is tuned to detect bright versus dark wakes based on visual assessment as input. Further work can be done in order to automate this process. Other methods can also be employed in order to overcome the apparent limitation of the Radon transform – the inability to detect curved ship wakes. Additionally, accurate velocity estimation of the ship cannot be carried out if the ship's heading is almost parallel to the cross-range direction, or if the pixel spacing is too large. More data testing could also be done to produce more robust  $N$  maxima and  $K$  values thresholds.

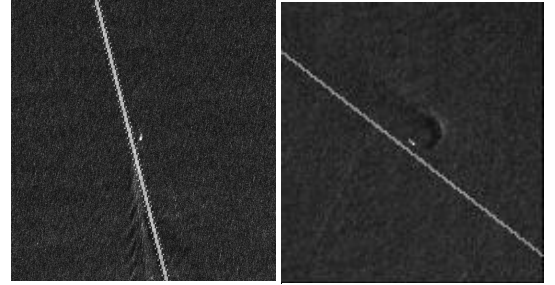


**Figure 17:** Chip with parallel ship heading.

**Figure 18:** Chip with curved wake.

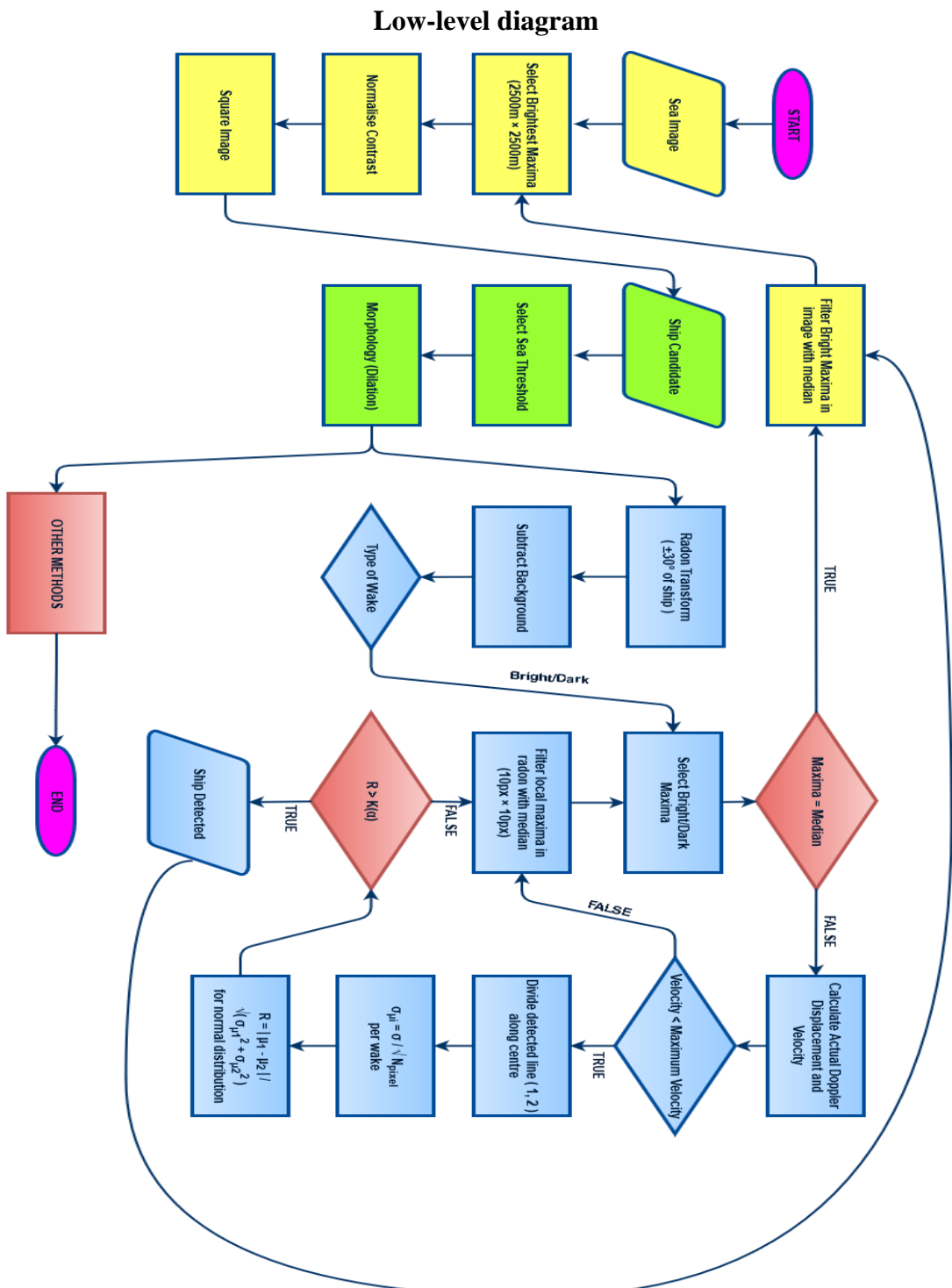
## 6 CONCLUSION

In a real-world scenario, it is inevitable to come across SAR images containing high noise levels, making it seemingly impossible to carry out ship wake detection. In this project, we worked to improve existing methods by incorporating innovative filters into the widely used Radon transform for ship wake detection in non-ideal SAR imagery. In terms of verification, the use of thresholds has proven necessary to reliably determine a wake's presence, or lack thereof. The constructed algorithm has, thus, succeeded in overcoming various noisy conditions that are inevitable in the real-world scenario, allowing for ship traffic surveillance to still be carried out.

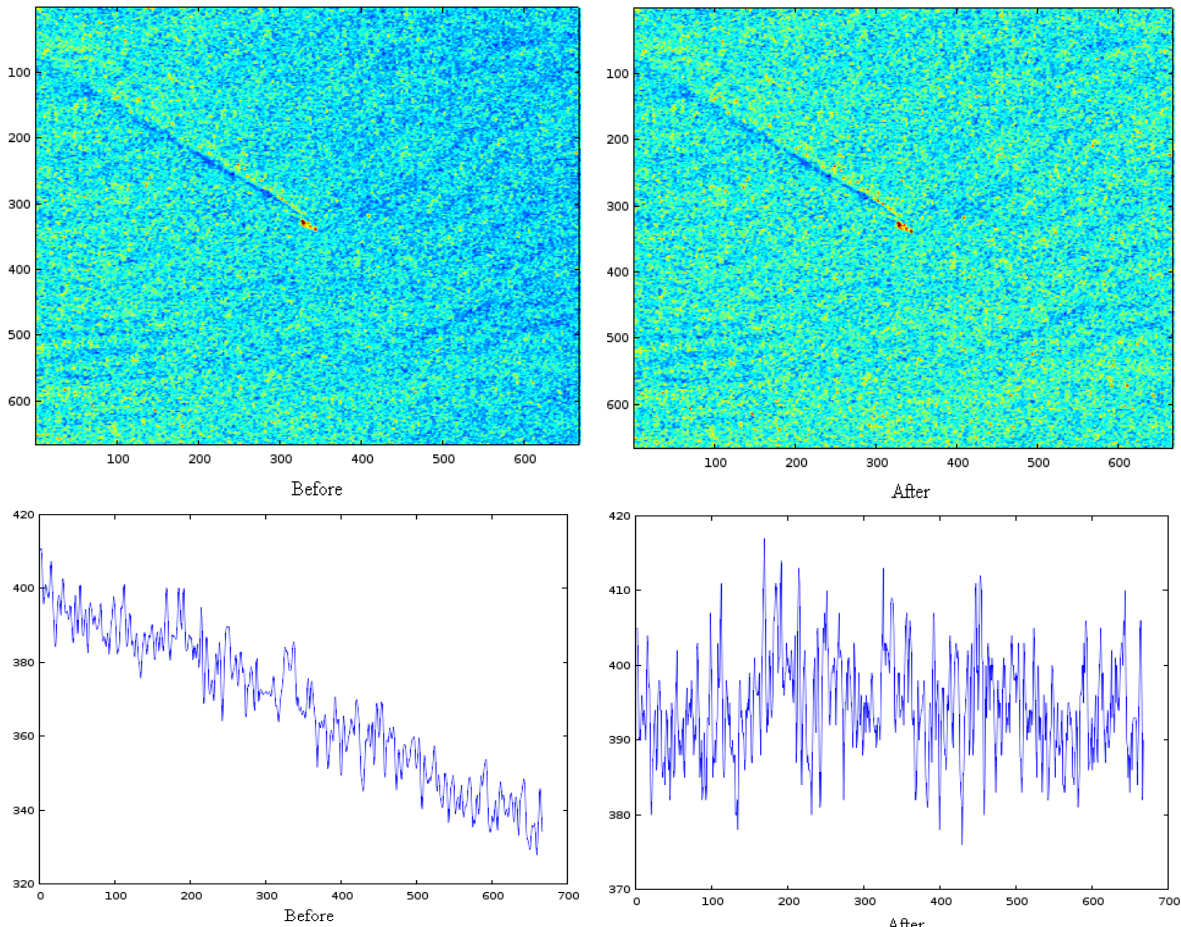
**REFERENCES**

- [1] Jackson, C. R., Apel, J. R., & United States. (2004). *Synthetic aperture radar: Marine user's manual*. Washington, D.C.: U.S. Dept. of Commerce, National Oceanic and Atmospheric Administration, National Environmental Satellite, Data, and Information Serve, Office of Research and Applications.
- [2] Eldhuset, K (1996): An automatic ship and ship wake detection system for spaceborne SAR images in coastal regions, *IEEE Trans on Geosc and Rem Sens Symp*, Vol. 34. No. 4, pp. 1009-1019.
- [3] Live Ships Map - AIS - Vessel Traffic and Positions | AIS Marine Traffic. (n.d.). Retrieved November 18, 2015, from <http://www.marinetraffic.com>
- [4] A. Scherbakov, R. Hanssen, G. Vosselman, R. Feron (23–26 September 1996). *Ship wake detection using Radon transforms of filtered SAR imagery*. Proc. European Symp. on Satellite Remote Sensing: Microwave Sensing and Synthetic Aperture Radar.
- [5] Manikas, A. (2015). *Beamforming: Sensor signal processing for defence applications* (5th ed.). Singapore [u.a.]: World Scientific, Imperial College Press.

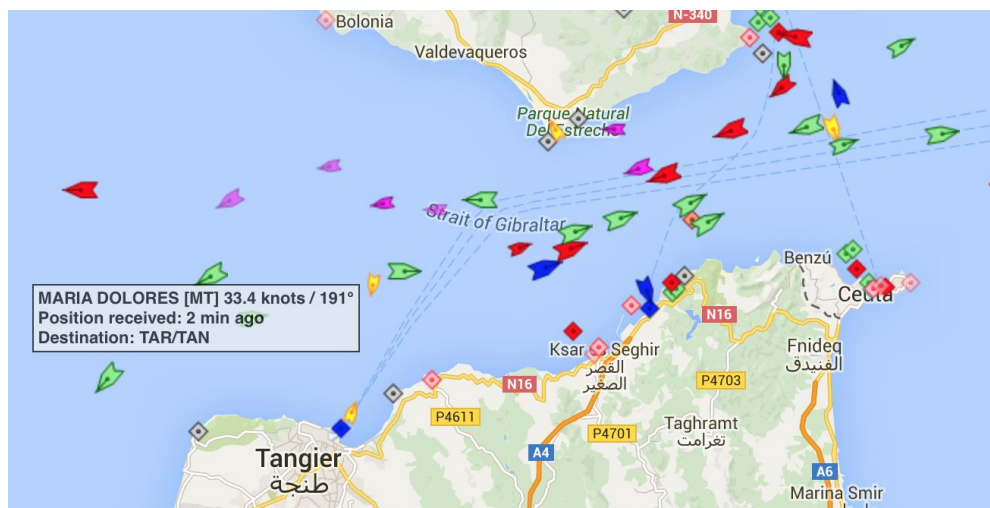
## APPENDIX



### Normalising Filter



Graph showing the medians of every column before and after the Normalising Filter.



Maximum ship velocity obtained from MarineTraffic [3].

**Scenario 1: Proximity Criterion**

Chip No.	Dark	Bright	Bearing / °	N	K	Velocity / ms <sup>-1</sup>	Notes (Visible)
1	✓		261	1	23.572	9.1395	Wake present
2	✓		258	1	26.673	5.775	Wake present
3	✓		259	1	42.413	7.7045	Wake present
4	✓		259	1	59.072	6.3646	Wake present
5	✓		249	1	20.471	9.5628	Wake present
6	✓		257	1	48.722	6.5501	Wake present
7	✓		257	3	50.646	6.2053	Wake present
8	✓		234	5	27.029	7.9304	Wake present
9		✓	236	1	9.3649	3.9787	Wake present
10		✓	341	1	80.399	12.092	Wake present
11		✓	350	1	99.252	24.023 (Rejected)	Wake present
12				9	2.4296		Noise
13				7	0.045187		Noise
14				7	1.4837		Noise
15				13	1.785		Noise
16				3	1.3507		Noise
17				1	1.2055		Noise
18				12	2.1572		Noise
19				1	2.344		Noise
20				6	0.0088912		Noise
21				2	5.8132		Noise

**Scenario 2: Normalising Filter + Proximity Criterion + Limited Angles**

Chip No.	Dark	Bright	Bearing / °	N	K	Notes
1	✓		301	2	60.047	Wake present
2	✓		304	2	4.7318	Long wake (covering entire side)
3	✓		320	2	30.173	Wake present
4	✓		312	3	38.962	Wake present
6	✓		310	6	7.2607	Weak wake
8	✓		310	4	48.531	Wake present
9	✓		314	2	20.107	Wake present
10	✓		323	5	25.212	Weak wake
11	✓		302	2	14.597	Wake present
12	✓		314	2	50.673	Wake present
13	✓		326	4	14.396	Weak wake
14	✓		316	9	NA	Wake present; Chip at edge of image
15	✓		322	3	34.671	Wake present
16	✓		313	3	46.723	Wake present
20	✓		316	2	62.741	Wake present
21	✓		322	3	14.857	Wake present
22	✓		312	2	11.266	Wake present
24	✓		320	3	38.602	Wake present
27	✓		314	2	26.664	Wake present
28	✓		322	2	18.793	Wake present
29	✓		313	2	42.714	Wake present
30	✓		316	3	3.8054	Weak wake
5			295	37	2.2594	No wake (ship is stationary)
7			196	24	NA	No wake; Chip at edge of image
17			304	9	5.9029	No wake (ship is stationary)
18			339	44	7.2152	Curved wake (ship is turning)
19			325	14	0.37059	No wake
23			183	8	2.2775	No wake (ship is stationary)
25			305	29	7.2827	Curved wake (ship is turning)
26			205	6	5.4211	No wake (ship is stationary)

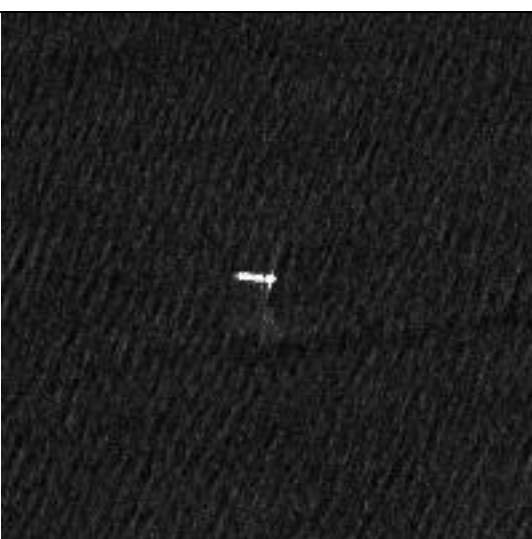
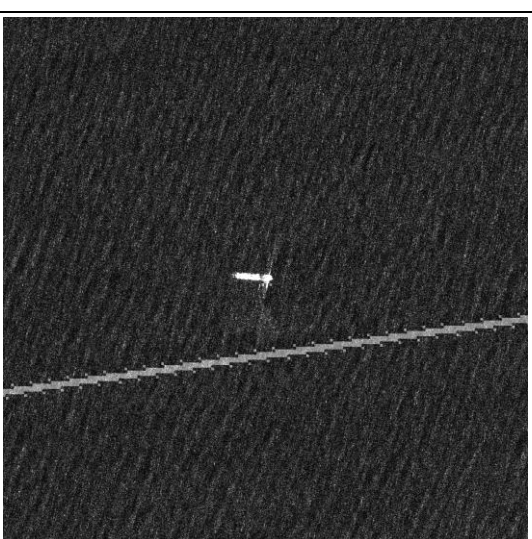
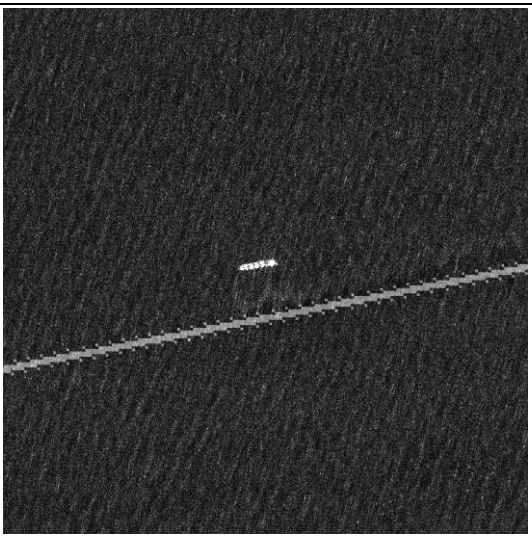
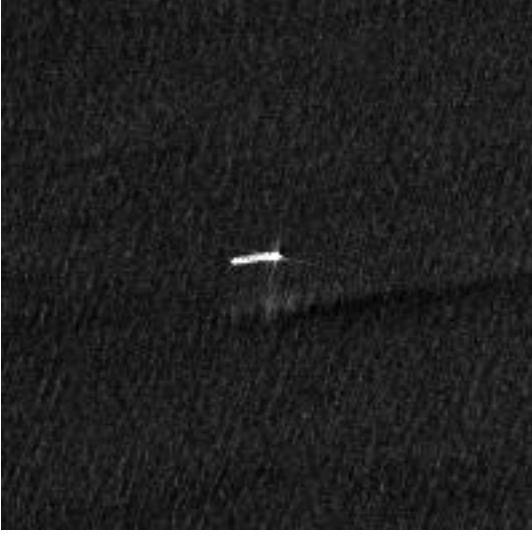
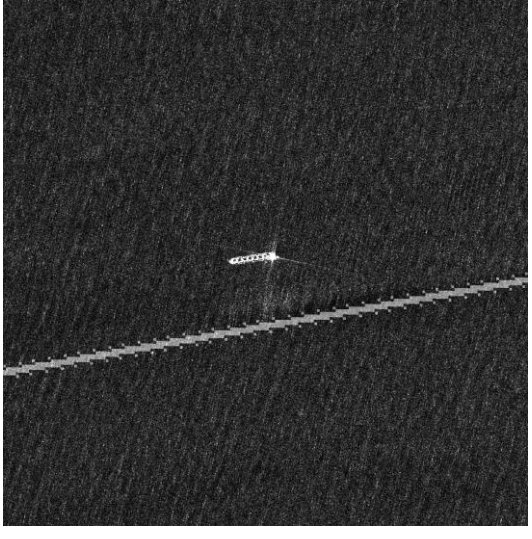
**Results showing addition of filters to Scenario 2**

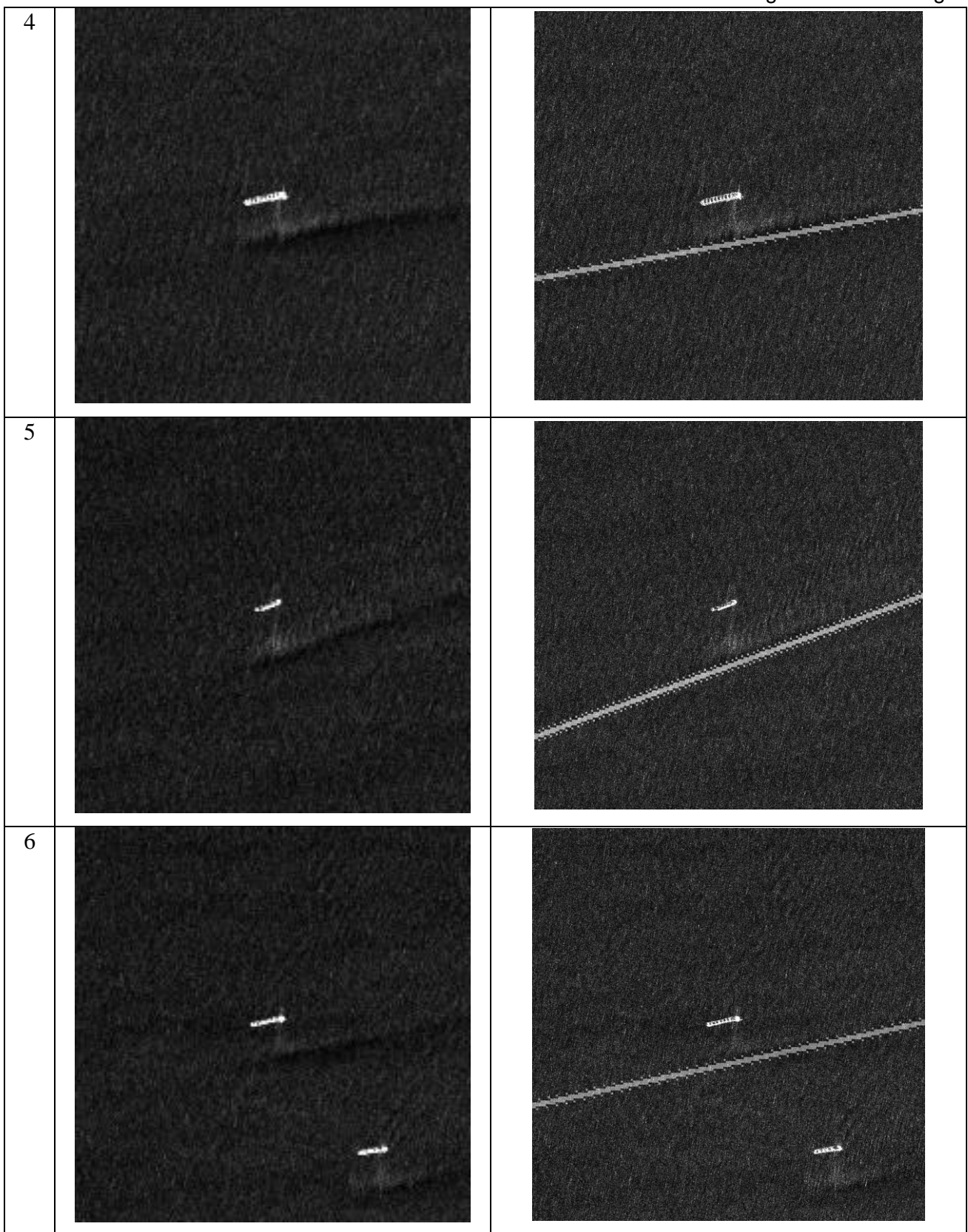
Stage A.	-				
Stage B.	Proximity Criterion				
Stage C.	Proximity Criterion + Limited Angles				
Stage D.	Proximity Criterion + Limited Angles + One-Dimensional				

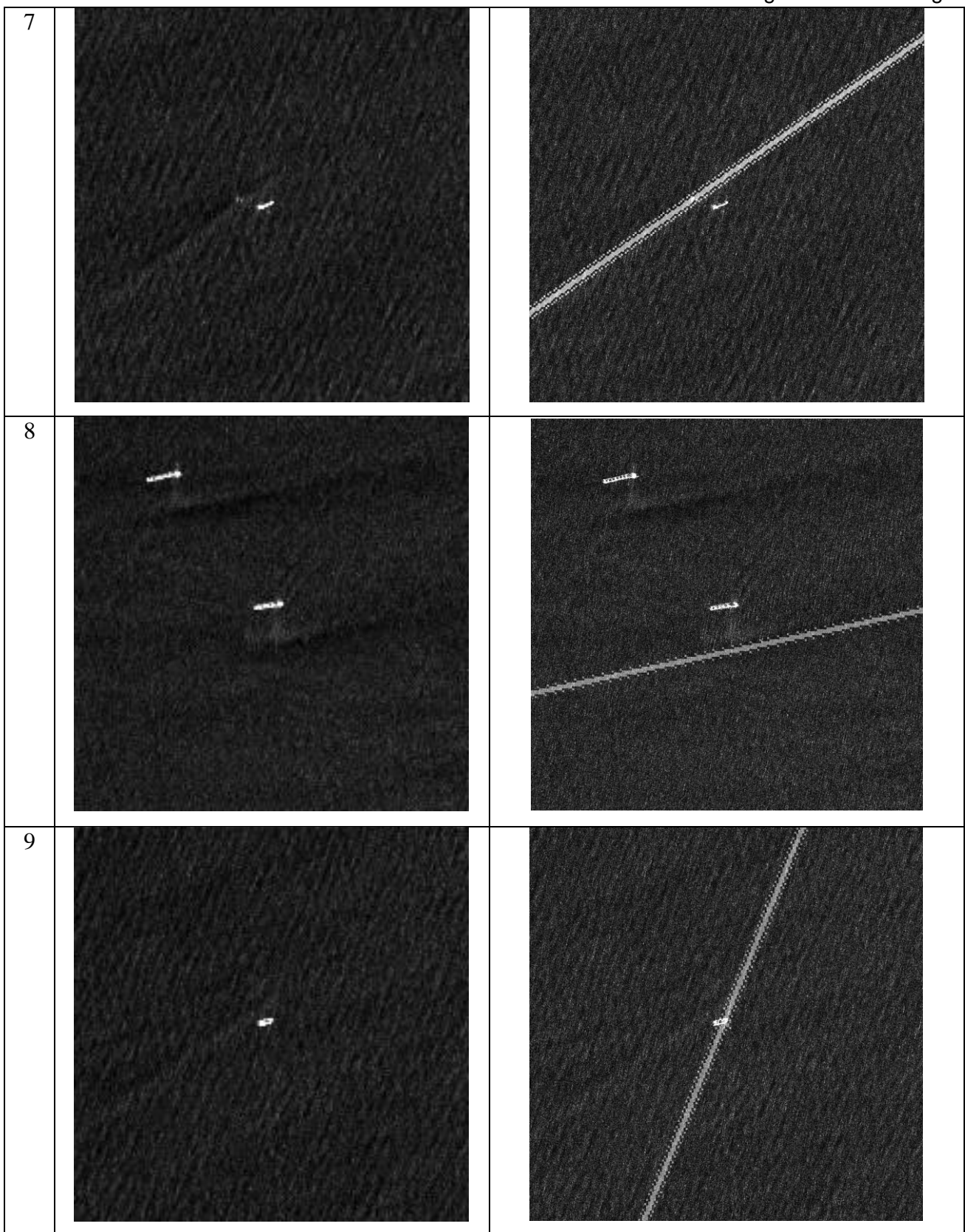
No.	B. Proximity		C. Proximity + Angle			D. 1D + Proximity + Angle					Notes	
	N	K	N	K	N	K	Bearing / °					
1	x	1	11.123	✓	4	60.047	✓	2	60.047	301	Dark	
2	✓	6	4.1163	✓	3	4.7318	✓	2	4.7318	304	Dark	Long
3	✓	15	31.398	✓	3	30.173	✓	2	30.173	320	Dark	
4	✓	20	34.156	✓	10	38.962	✓	3	38.962	312	Dark	
6	x	7	8.5355	✓	6	7.2607	✓	6	7.2607	310	Dark	Weak
8	✓	50	46.283	✓	5	48.531	✓	4	48.531	310	Dark	
9	x	1	35.706	✓	3	20.107	✓	2	20.107	314	Dark	
10	x	19	10.681	✓	8	25.212	✓	5	25.212	323	Dark	Weak
11	✓	25	14.595	x	27	36.388	✓	2	14.597	302	Dark	Turning
12	✓	34	51.546	✓	13	50.673	✓	2	50.673	314	Dark	
13	✓	19	13.141	✓	19	14.396	✓	4	14.396	326	Dark	Weak
14	✓	41	NA	x	9	NA	✓	9	NA	316	Dark	Edge
15	✓	38	38.087	✓	18	34.671	✓	3	34.671	322	Dark	
16	✓	16	46.018	✓	9	46.723	✓	3	46.723	313	Dark	
20	✓	28	64.658	✓	3	62.741	✓	2	62.741	316	Dark	
21	x	28	34.869	✓	9	14.857	✓	3	14.857	322	Dark	Artifact
22	x	76	38.015	✓	28	11.266	✓	2	11.266	312	Dark	Turning
24	✓	40	41.445	✓	7	38.602	✓	3	38.602	320	Dark	
27	✓	32	19.803	✓	9	24.406	✓	2	26.664	314	Dark	
28	✓	5	19.034	✓	2	18.793	✓	2	18.793	322	Dark	
29	✓	33	44.666	✓	9	42.714	✓	2	42.714	313	Dark	
30	✓	7	0.033655	✓	4	3.8054	✓	3	3.8054	316	Dark	Weak
5	NA	9	4.5289	NA	27	11.325	NA	37	2.2594	295	NA	
7	NA	44	NA	NA	26	NA	NA	24	NA	196	Dark	Edge
17	NA	27	11.342	NA	11	5.9029	NA	9	5.9029	304	NA	
18	NA	15	36.394	NA	FAILED PROX.		NA	44	7.2152	339	Dark	Curved
19	NA	31	0.75415	NA	15	9.6393	NA	14	0.37059	325	Dark	Weak

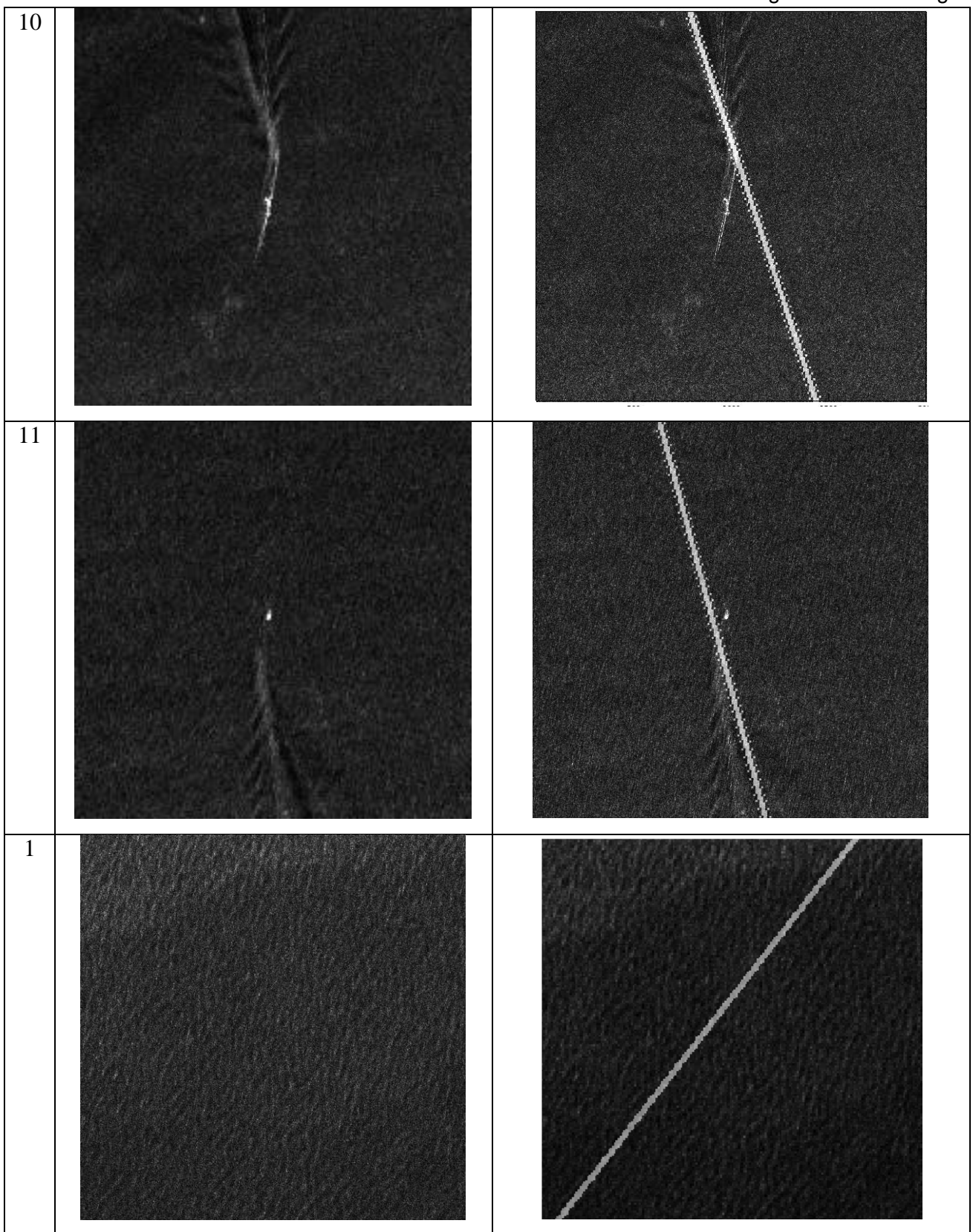
23	NA	15	8.2749	NA	8	2.2775	NA	8	2.2775	183	NA	
25	NA	36	40.669	NA	25	7.7696	NA	29	7.2827	305	Dark	Curved
26	NA	10	10.516	NA	9	5.4211	NA	6	5.4211	205	NA	

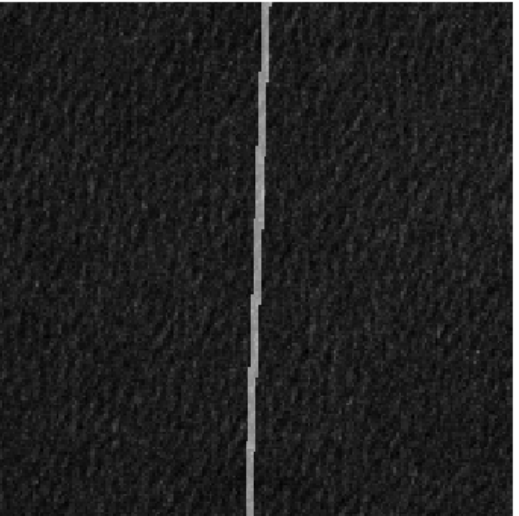
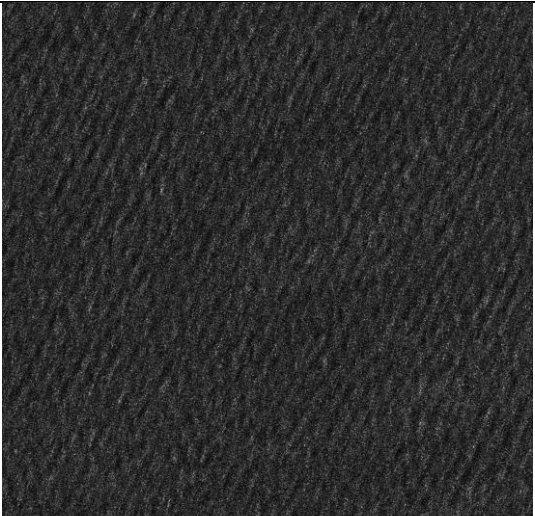
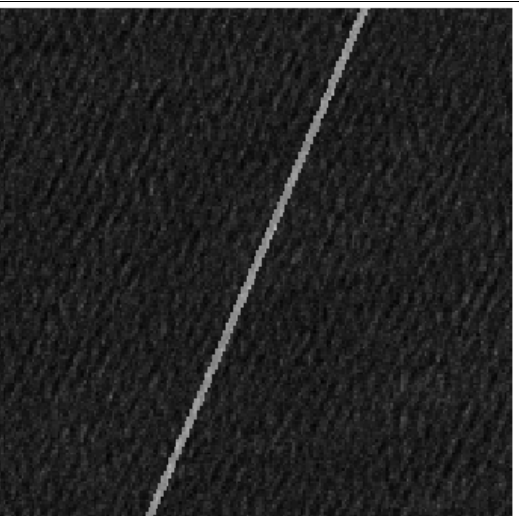
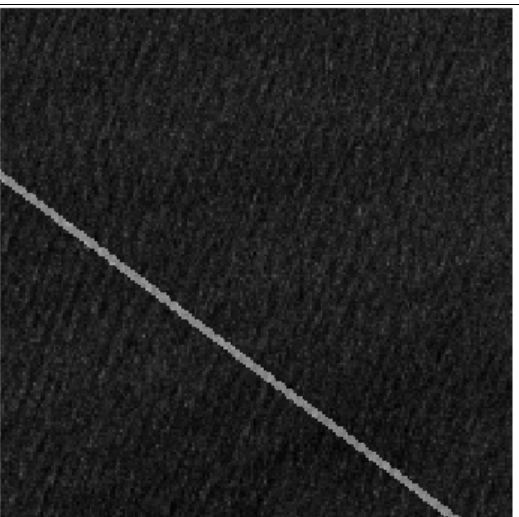
**Chips from Scenario 1**

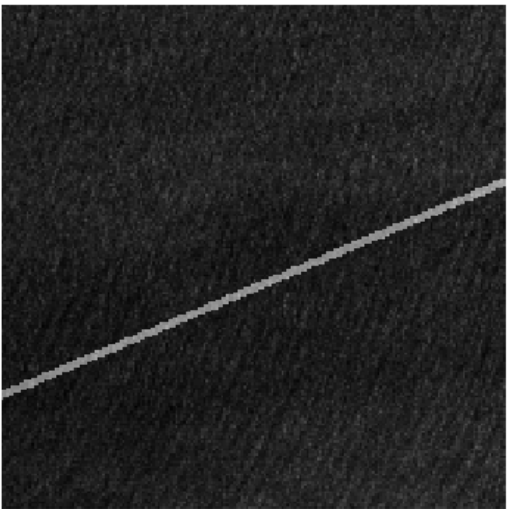
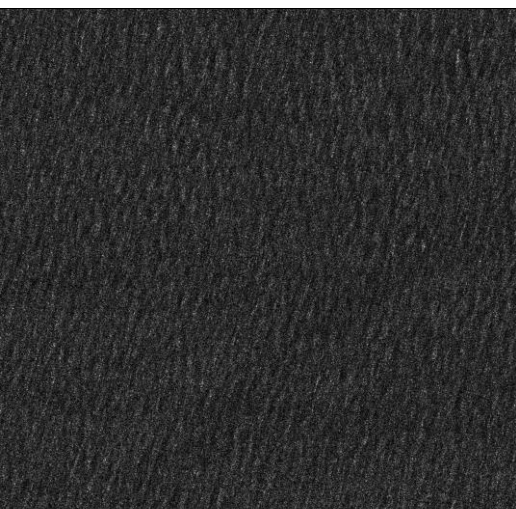
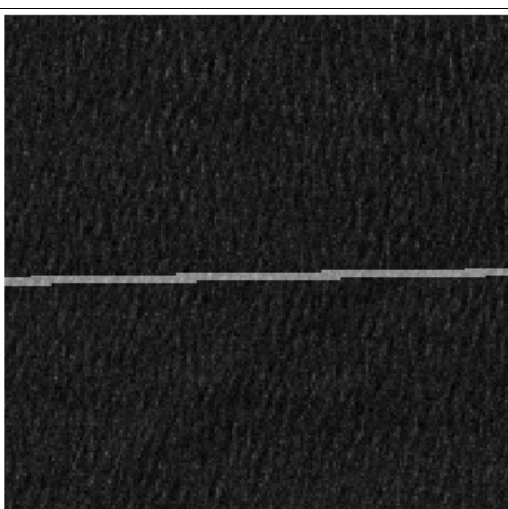
No	Original	With Wake
1		
2		
3		

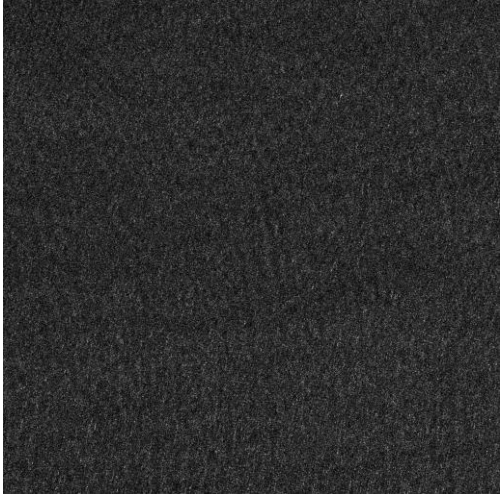
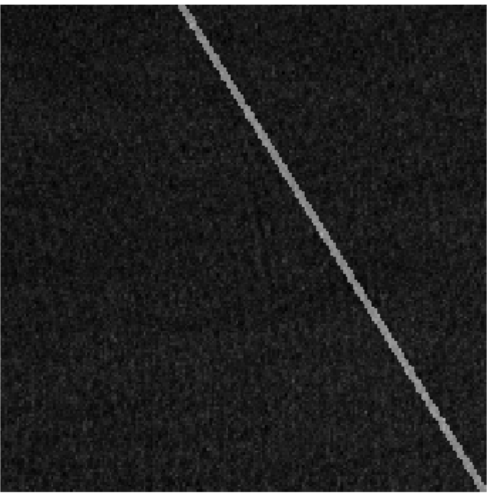
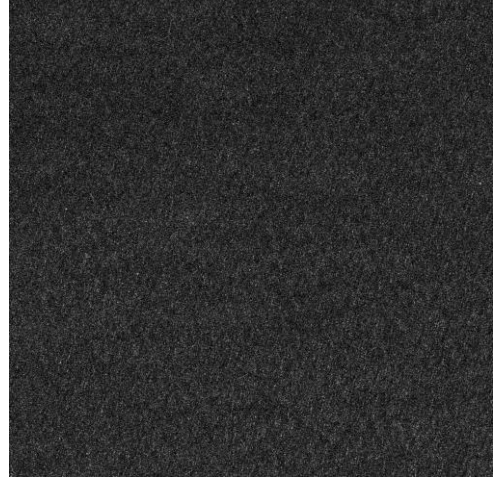
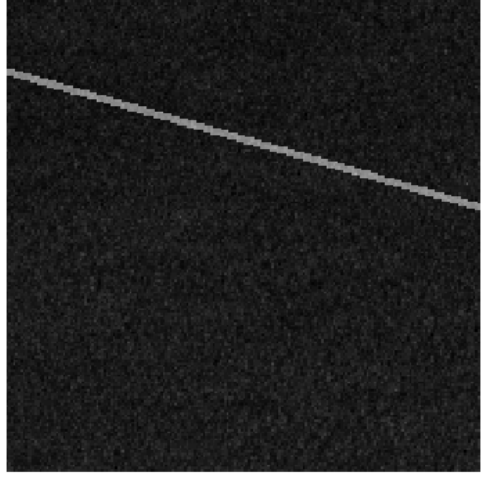
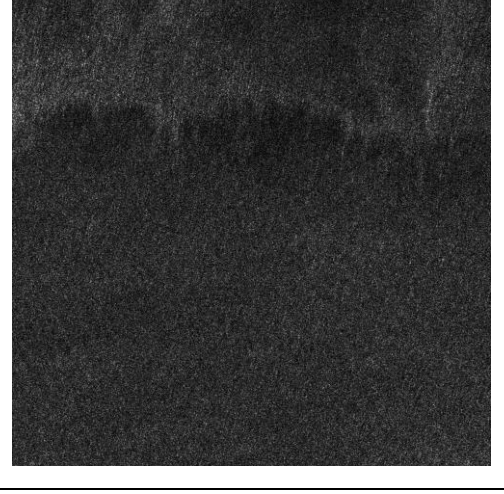




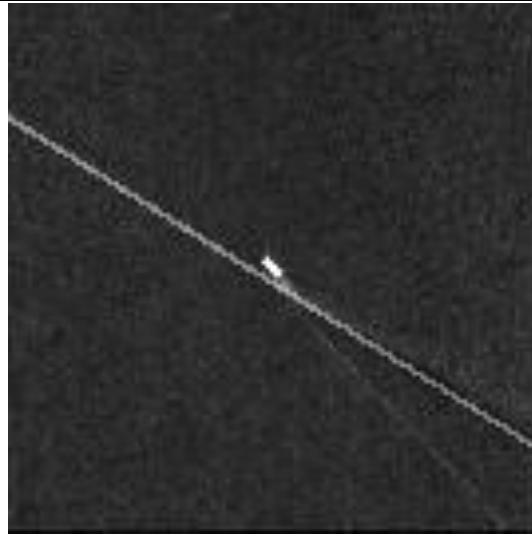
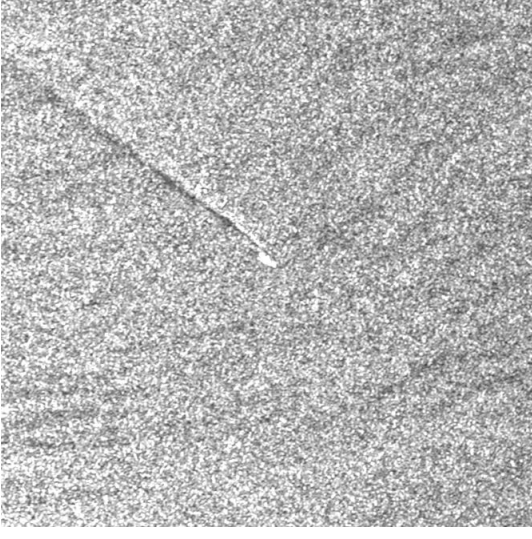
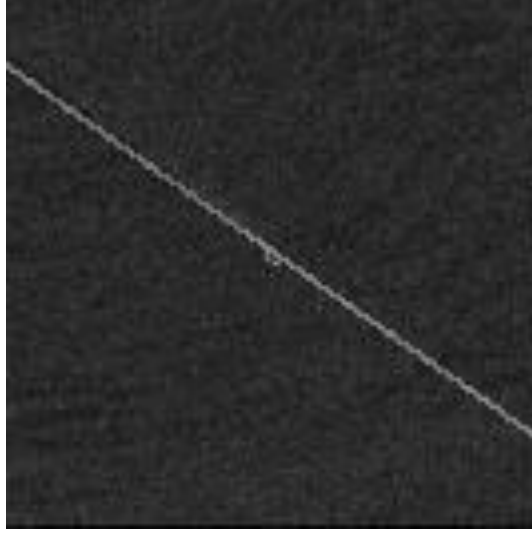
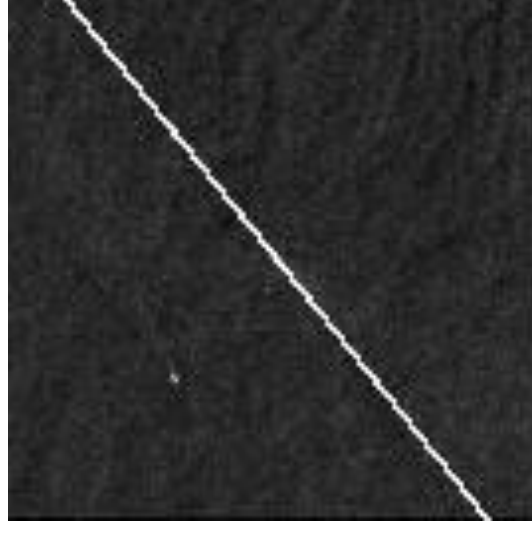


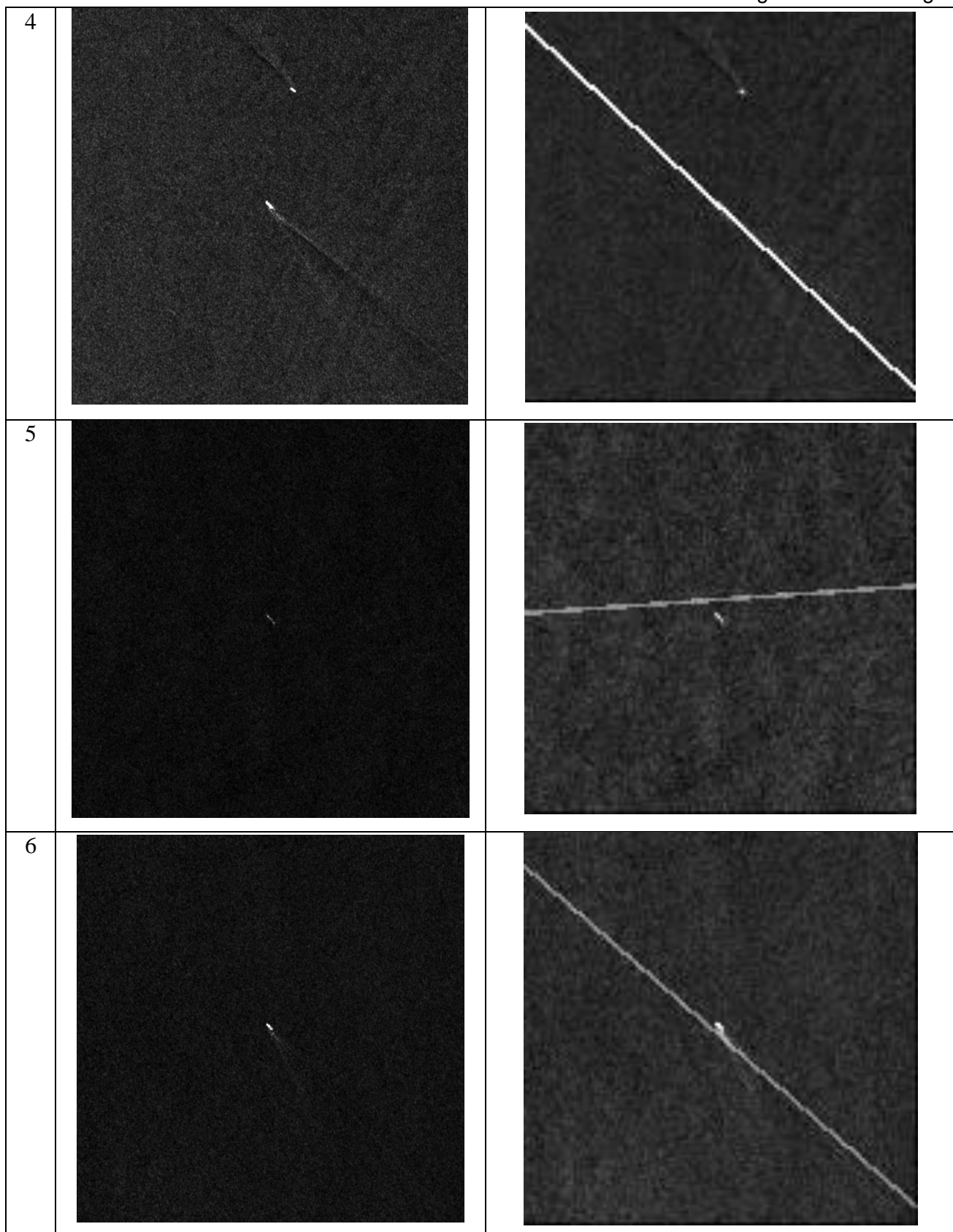
2		
3		
4		

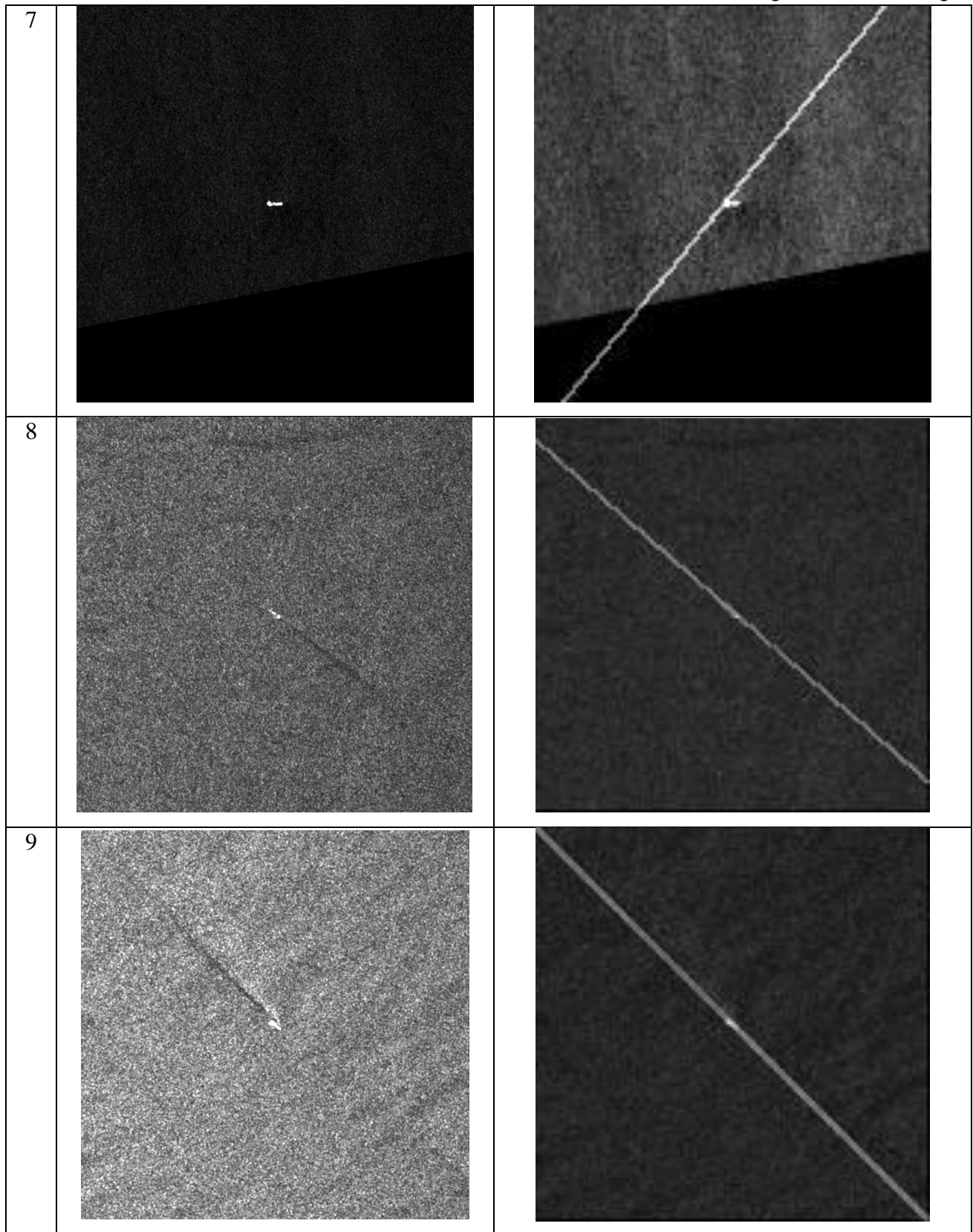
5		
6		
7		

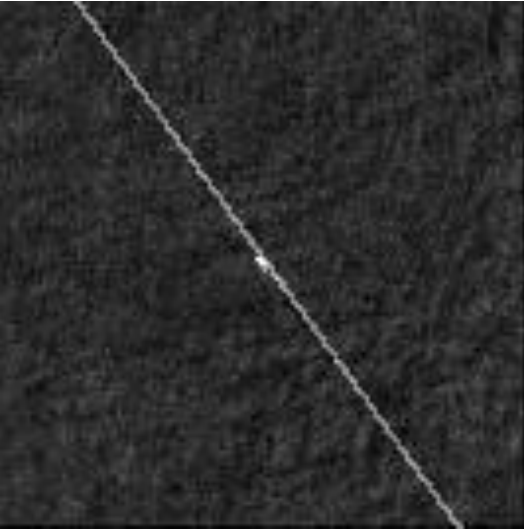
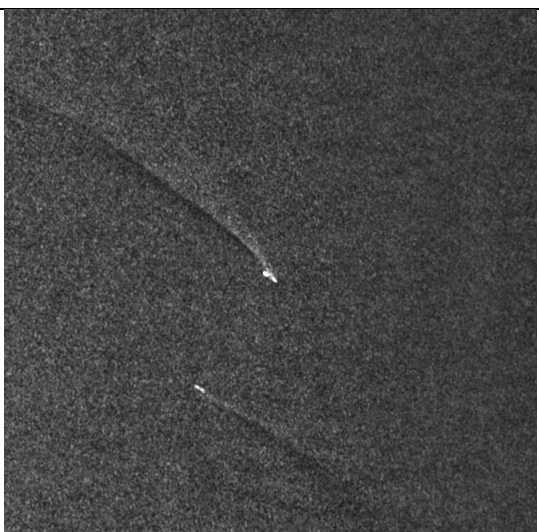
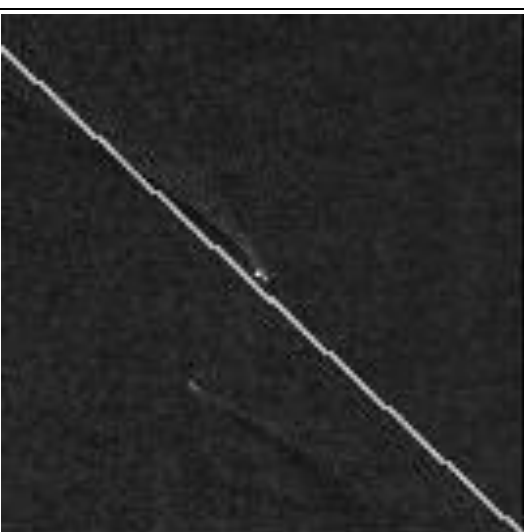
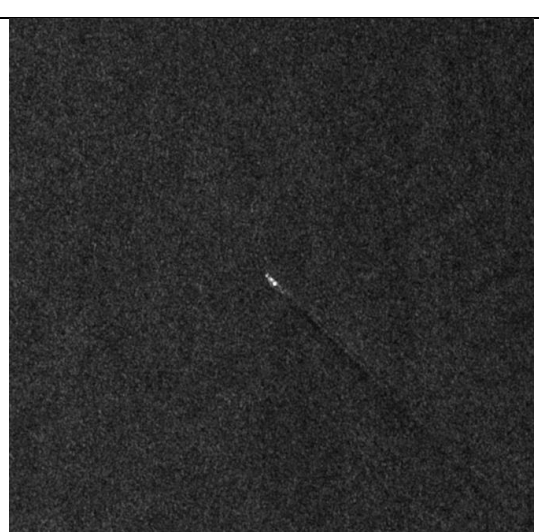
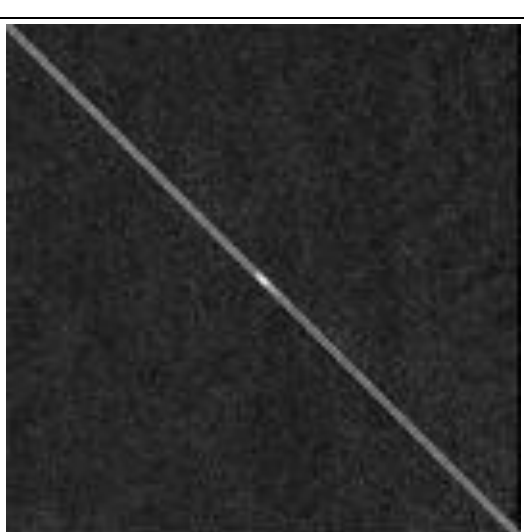
8		
9		
10		

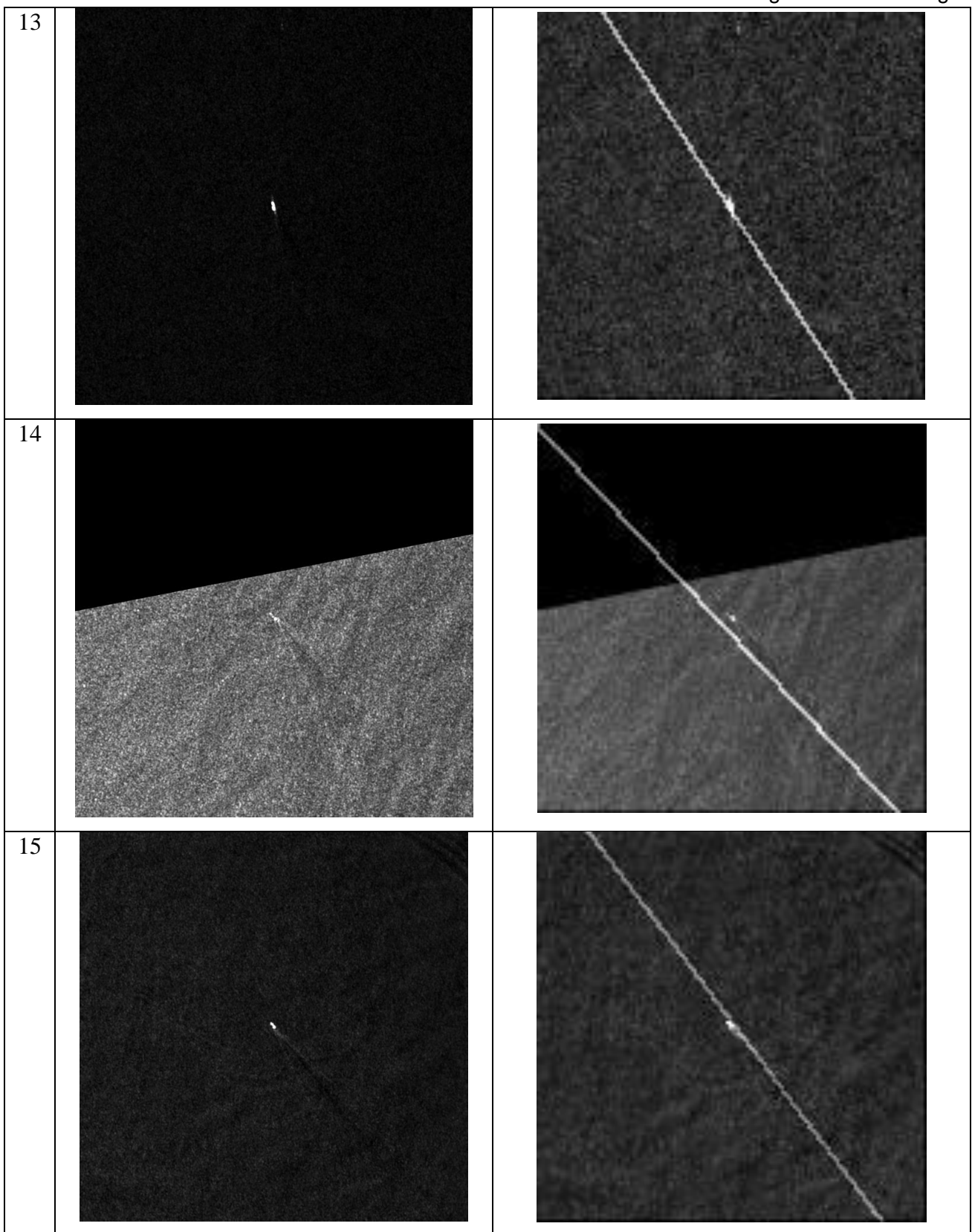
**Chips from Scenario 2**

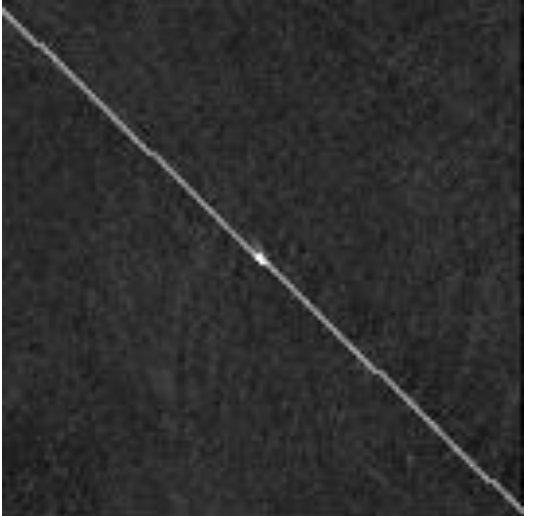
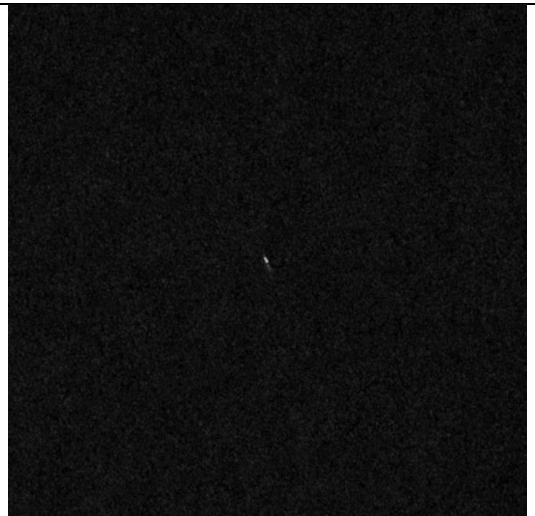
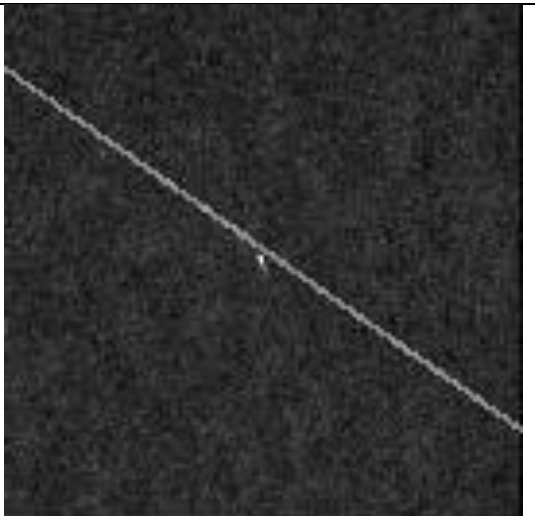
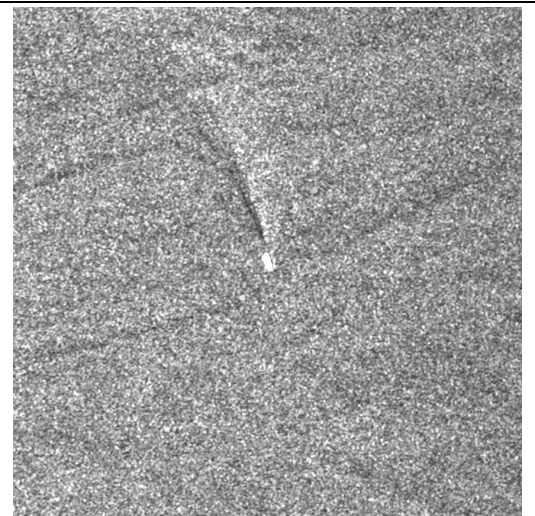
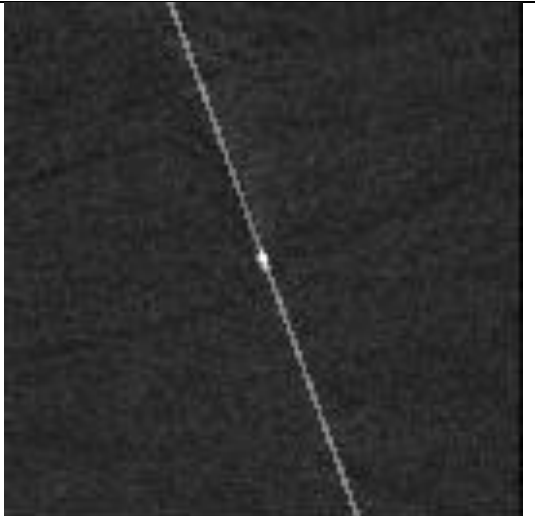
No	Original	With Wake
1		
2		
3		

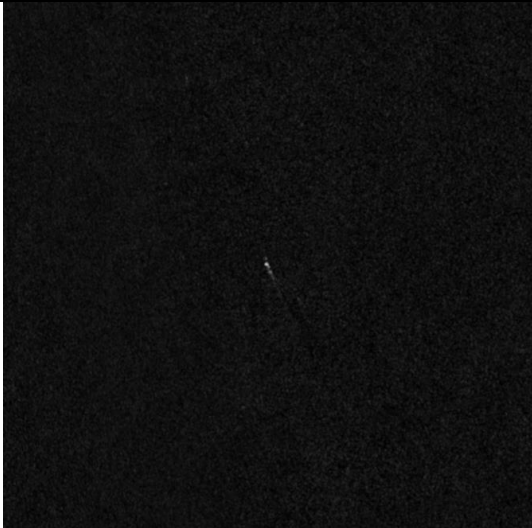
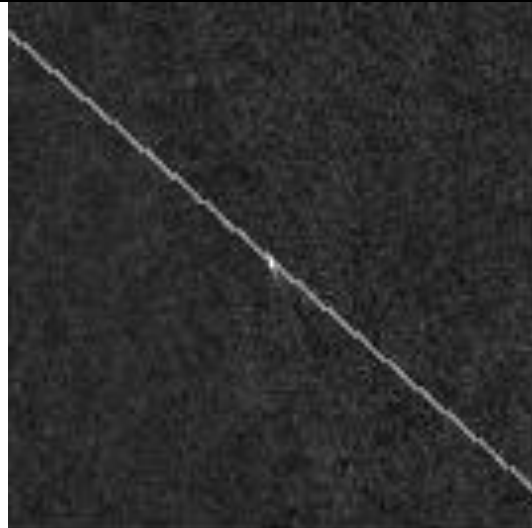
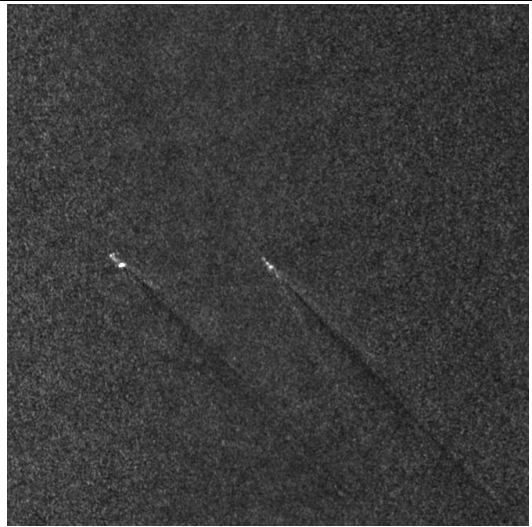
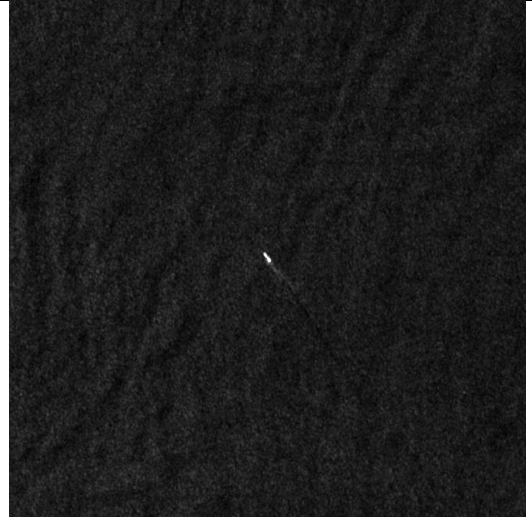
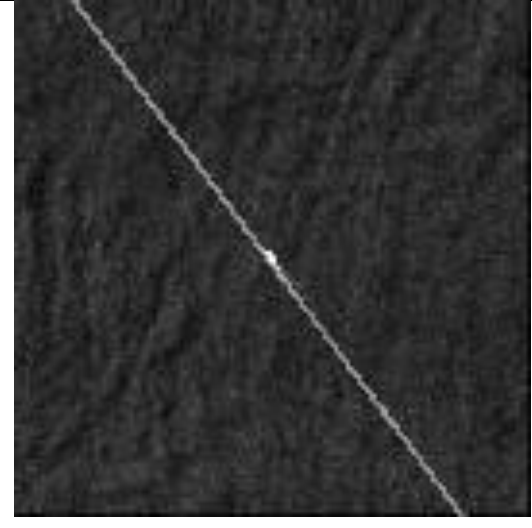


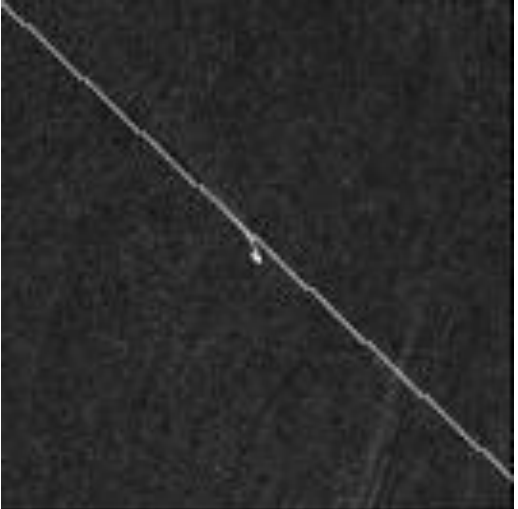
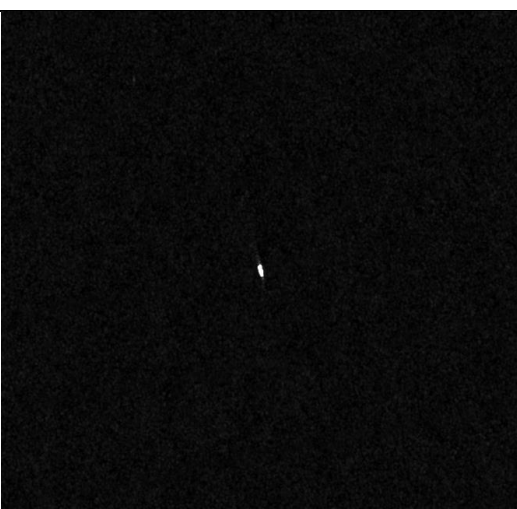
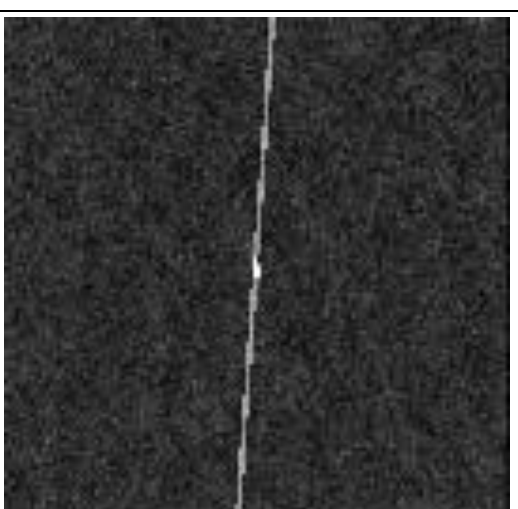
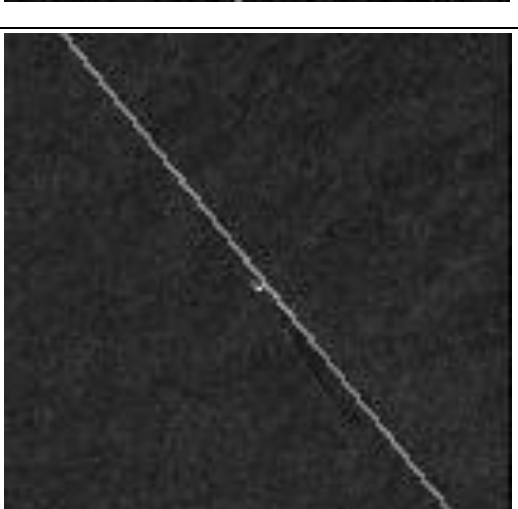


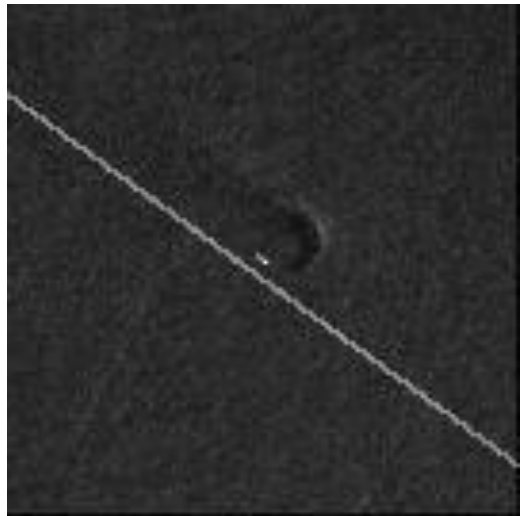
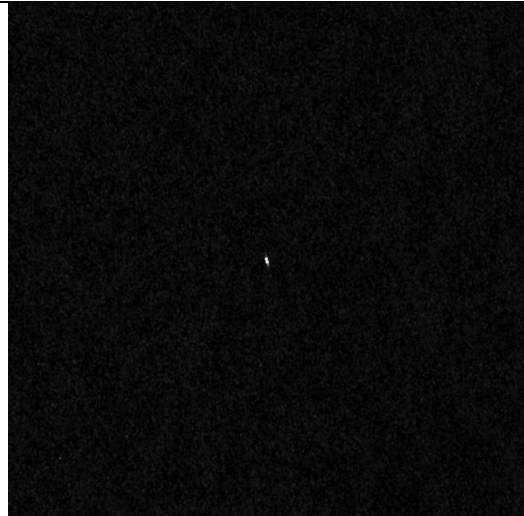
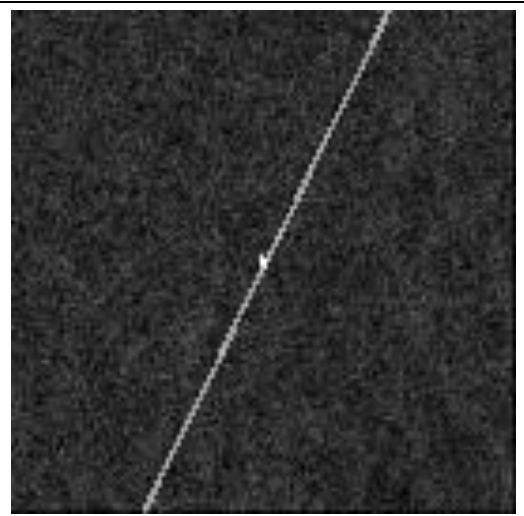
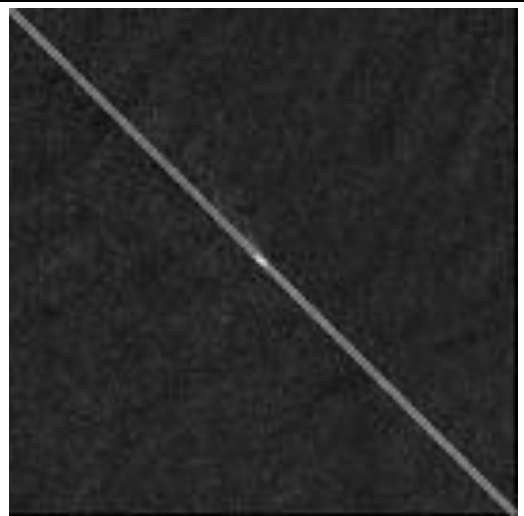
10		
11		
12		

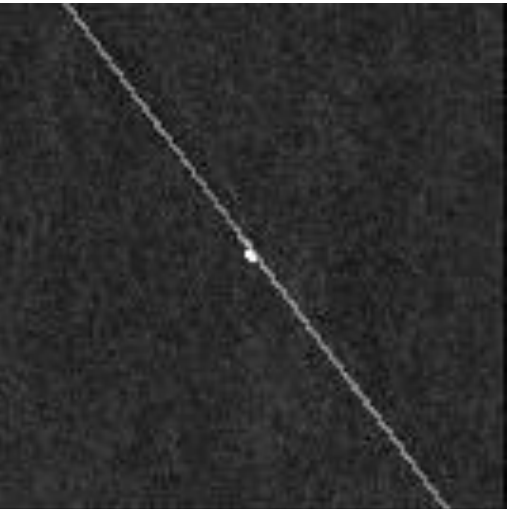
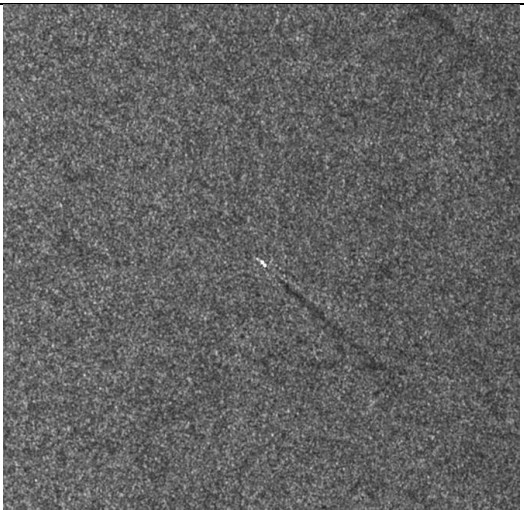
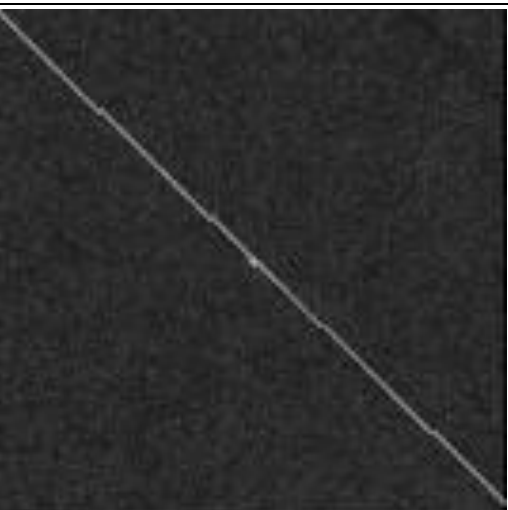


16		
17		
18		

19		
20		
21		

22		
23		
24		

25		
26		
27		

28		
29		
30		